

Magnetic Skyrmion Encoding by Structured Light

Qifan Zhang^{1,2,3}, Wangke Yu⁴, Zhongquan Nie⁶, Yijie Shen^{4,5,*} and Shirong Lin^{1,2,†}

¹*School of Physical Sciences, Great Bay University, Dongguan 523000, China*

²*Great Bay Institute for Advanced Study, Dongguan 523000, China*

³*School of Physics and Materials Science, Guangzhou University, Guangzhou 510006, China*

⁴*Centre for Disruptive Photonic Technologies, School of Physical and Mathematical Sciences, Nanyang Technological University, Singapore 637371, Singapore*

⁵*School of Electrical and Electronic Engineering, Nanyang Technological University, Singapore 639798, Singapore*

⁶*National University of Defense Technology, College of Advanced Interdisciplinary Studies, Changsha 410073, China*

Structured light fields, featuring unique topological properties and high tunability, have opened new frontiers in light-matter interactions with magnetic systems. However, the ultrafast and reconfigurable optical encoding of various types of topological magnetic textures remains a significant challenge. Here, we systematically investigate the encoding mechanism of structured light in magnets via the higher-order Poincaré sphere. By uncovering the precise relationship between the winding number of structured light and the topological charge of magnetic textures, we establish a fundamental topological connection between light and magnetism. This framework enables ultrafast, all-optical encoding of diverse topological spin textures in magnetic media, including skyrmions, antiskyrmions and skyrmion bags. Our work advances the fundamental understanding and all-optical control of topological magnetism, offering a promising route for designing skyrmion-based devices.

Introduction—Structured light [1–14], owing to its diverse topological properties and high degree of controllability, holds immense potential not only for fundamental studies but also in the field of light-controlled magnetism [15–29], particularly in the manipulation of magnetic topological textures such as magnetic skyrmions [30–41]. Magnetic skyrmions are topological spin textures in real space [42–50], and are characterized by their small size [51–54], versatile generation [55–68] and manipulation methods [69–81]. Additionally, skyrmions exhibit fluidity, enabling multiple skyrmions to form skyrmion bags [82–88]. In the field of information storage, skyrmions demonstrate significant application potential [89–94].

In 2017, it was shown that circularly polarized vortex light can controllably generate magnetic skyrmions in chiral magnets [31]. Recently, our group revealed the mechanism whereby vortex light generates a specific number of magnetic skyrmions, determined by the angular momentum and amplitude of light [32]. Yet, research on generating skyrmions with structured light needs expansion in breadth (to diverse polarizations and materials) and depth (mechanism). A key limitation is the lack of a defined angular momentum for beams with arbitrary polarization patterns. To our knowledge, a significant gap exists in both applying such structured light to encode skyrmions and in understanding the corresponding mechanisms. In 2011, Milione et al. proposed the higher-order Poincaré sphere (HOPS) to describe the higher-order polarization states of vector vortex beams [4]. The model provides a concise, unified framework for struc-

tured light-matter interactions, offering new perspectives for light-controlled magnetism.

Here, we investigate the encoding of magnetic topological textures in ferromagnetic thin films using topological HOPS structured light. We develop a light-magnet coupling model in which the structured light’s magnetic field is incorporated via the Zeeman effect (Our model also applies to light’s electric field in multiferroics via magneto-electric coupling [31]), and simulate magnetization dynamics with the Landau–Lifshitz–Gilbert (LLG) equation. The light’s magnetic field exhibits topological features quantified by a winding number. Through interaction with the magnetic medium, controlled encoding of skyrmions, antiskyrmions, and skyrmion bags is achieved in magnet with different Dzyaloshinskii–Moriya interaction (DMI) types. The topology of encoded textures correlates with the winding number, highlighting implications for light-controlled skyrmionics.

Model—The north and south poles of the HOPS represent two orthogonal circularly polarized vortex eigenstates carrying opposite topological charges, which constitute the fundamental components of any state of polarization in the sphere. The amplitude distribution of the magnetic fields of structured beams on the poles of HOPS can be expressed as

$$B(\mathbf{r}, t) = B_0 \frac{A_m(\mathbf{r})}{\max_{\mathbf{r}} |A_m(\mathbf{r})|} e^{(-\frac{(t-t_0)^2}{\sigma^2} - i\omega t)}. \quad (1)$$

Here, A_m is the amplitude distribution of the magnetic field generated by the Laguerre–Gaussian beam, m the value of orbital angular momentum (OAM) and also the order of the HOPS, B_0 the magnetic field strength coefficient, ω the light frequency, t_0 the time at which the magnetic field strength reaches its maximum within one

* yijie.shen@ntu.edu.sg

† shironglin@gbu.edu.cn

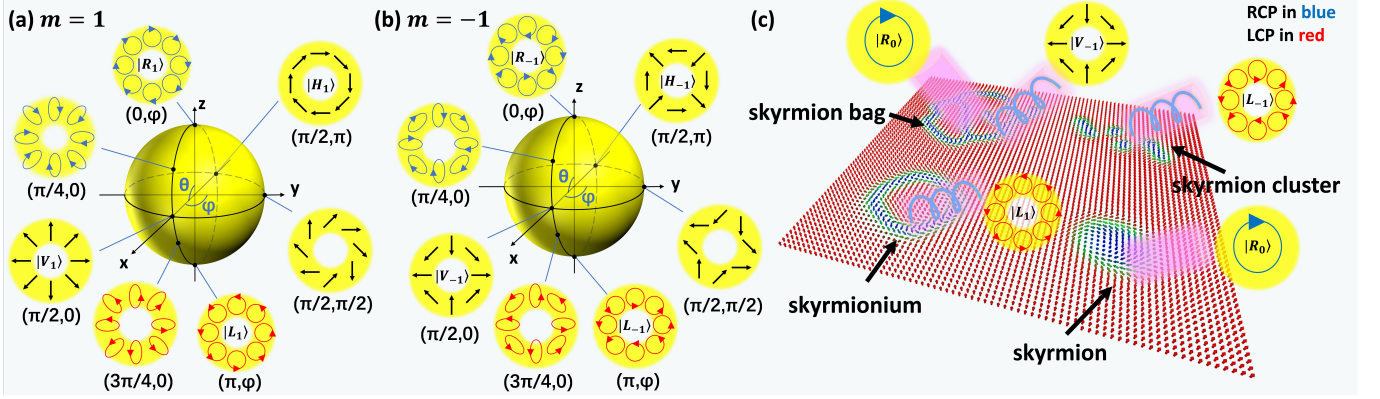


FIG. 1. Representation of the higher-order Poincaré sphere (HOPS) for (a) $m = 1$ and (b) $m = -1$. Representative polarization states at selected (θ, φ) points are illustrated. The poles correspond to circularly polarized vortex eigenstates, the equator corresponds to π -vector beams, and intermediate points correspond to elliptically polarized states. (c) Schematic illustration of magnetic textures encoded by HOPS structured light.

period, and σ the pulse duration. We work in the paraxial regime and consider only the transverse magnetic-field components $\mathbf{B} = B(\mathbf{r}, t)\mathbf{e}_p$, where $\mathbf{e}_p = \hat{\mathbf{x}} \pm i\hat{\mathbf{y}}$. Here we construct a time-localized pulse by multiplying the monochromatic HOPS field at a carrier frequency (ω) by a Gaussian temporal envelope [31, 32].

In the following analysis, we let θ and φ denote the latitude and longitude angles on the HOPS, Θ the azimuthal angle in the beam cross section and m the topological charge, which also indicates the order of the HOPS. Any point on the sphere corresponds to a polarization state that can be expressed as a linear superposition of the two eigenstates. This relationship can be described by the following two-dimensional Jones vector [4]:

$$|\rho\rangle = \cos\left(\frac{\theta}{2}\right)e^{-i\varphi}|R_m\rangle + \sin\left(\frac{\theta}{2}\right)|L_m\rangle, \quad (2)$$

with respect to the orthonormal circular polarization basis $\{R_m, L_m\}$ such that $|R_m\rangle = \exp(-im\Theta)(\hat{\mathbf{x}} + i\hat{\mathbf{y}})$ and $|L_m\rangle = \exp(im\Theta)(\hat{\mathbf{x}} - i\hat{\mathbf{y}})$. From Equations (2), we obtain the expression for the magnetic field distribution from a HOPS structured beam with order m as follows:

$$\begin{aligned} |\mathbf{B}_m\rangle = & \cos\left(\frac{\theta}{2}\right)[e^{-i(m\Theta+\varphi)}, ie^{-i(m\Theta+\varphi)}]^T \\ & + \sin\left(\frac{\theta}{2}\right)[e^{im\Theta}, -ie^{im\Theta}]^T. \end{aligned} \quad (3)$$

According to Equation (3), we observe that each term contains $m\Theta$. This indicates that, for the HOPS structured beam with order m , along a closed path around the optical vortex in the transverse plane (Θ from 0 to 2π), the beam's complex amplitude accumulates a total phase Φ , which is $2\pi \cdot m$. The topological properties of the magnetic field distributions from the HOPS structured beam with order m can be characterized using a winding number, which is calculated by the following formula [5]:

$$l = \frac{1}{2\pi} \oint_C \nabla \Phi \cdot ds, \quad (4)$$

where C is a circular closed loop enclosing the vortex center, and ds is the path element along C . From Fig. 1 (a) and (b), as the azimuthal angle Θ varies from 0 to 2π around the center, the instantaneous magnetic polarization direction rotates accordingly. The number and direction (counterclockwise/clockwise) of rotations determine the absolute value and sign (+/−) of the winding number. Therefore, the magnetic field distributions generated by all light beams on the same HOPS structured beam with order m share identical topological properties.

Here, we focus on the HOPSS for $m = 1$ and $m = -1$, as shown in Fig. 1 (a) and (b), respectively. The plots display the magnetic field distributions of light corresponding to several representative points on the spheres.

For example, when $\theta = \pi/2$, it corresponds to π -vector beams on the equator: When $m = 1$ and $\varphi = 0$, according to Equations (3) and (4), $|\mathbf{B}_1\rangle = [\cos\Theta, \sin\Theta]^T$ and $l = 1$. In this case, the magnetic field distribution remains radial and appears as a single continuous annular domain without polarization segmentation. When $\varphi \neq 0$, the magnetic field direction remains oriented at an angle of $\varphi/2$ relative to the radial direction and appears as a similar distribution. For $m = -1$ and $\varphi = 0$, $|\mathbf{B}_{-1}\rangle = [\cos\Theta, -\sin\Theta]^T$ and $l = -1$. In this case, the polarization toggles between outward and inward radial direction every $\pi/2$ in azimuth, completing four reversals in a full circle. Since the magnetic polarization in the transitional region forms a vortex distribution during each alternation, four vortex configurations of polarization emerge overall. When $\varphi \neq 0$, the magnetic field direction at each position is rotated by $\varphi/2$, but the overall magnetic field distribution retains a similar configuration. With multiple vortex regions resembling skyrmion in-plane moments, these field configurations enable multi-skyrmion encoding in magnets.

Particularly, when $\theta = 0$ and π , it corresponds to right-hand polarized (RCP) and left-hand polarized (LCP) beams on the poles. Notably, their magnetic fields are

topologically similar to equatorial beams. Though locally rotating, each instantaneous distribution matches a specific equatorial case [32].

When $\theta \neq 0, \pi/2$ or π , the HOPS beam corresponds to elliptically polarized beam on the spherical surface (excluding the equator and the poles). Still, they remain topologically similar to equatorial beams. Elliptically polarized beams exhibit local magnetic field rotation (with time-varying amplitude), yet maintain an overall distribution akin to circularly polarized beams.

Figure 1(c) schematically illustrates the light-magnet interaction. We numerically investigate the influence of the magnetic fields of the HOPS structured beams with order $m = \pm 1$ on two distinct types of DMI magnets that respectively host Bloch-type skyrmions and antiskyrmions. We consider a ferromagnetic system comprising 201×201 lattice sites under periodic boundary conditions. The initial magnetic moment at each lattice site is set to $(0, 0, 1)$. The Hamiltonian is given by

$$H = -J \sum_{\mathbf{r}} \mathbf{m}_{\mathbf{r}} \cdot (\mathbf{m}_{\mathbf{r}+a\mathbf{e}_x} + \mathbf{m}_{\mathbf{r}+a\mathbf{e}_y}) + D \sum_{\mathbf{r}, i} \mathbf{e}_i \cdot (\mathbf{m}_{\mathbf{r}} \times \mathbf{m}_{\mathbf{r}+a\mathbf{e}_i}) - H_z \sum_{\mathbf{r}} \mathbf{m}_z - \sum_{\mathbf{r}} \mathbf{B}(\mathbf{r}, t) \cdot \mathbf{m}_{\mathbf{r}}. \quad (5)$$

Here, J , D and H_z represent the exchange constant, the DMI constant and the constant external magnetic field applied along the z axis, a the lattice constant, \mathbf{e}_i the unit vector oriented along either the x or y axis. Two types of DMI Hamiltonian that generate Bloch-type and antiskyrmions are respectively given by $H_{DMI} = D \sum_{\mathbf{r}, i} \mathbf{e}_x \cdot (\mathbf{m}_{\mathbf{r}} \times \mathbf{m}_{\mathbf{r}+a\mathbf{e}_x}) + D \sum_{\mathbf{r}, i} \mathbf{e}_y \cdot (\mathbf{m}_{\mathbf{r}} \times \mathbf{m}_{\mathbf{r}+a\mathbf{e}_y})$ and $D \sum_{\mathbf{r}, i} \mathbf{e}_x \cdot (\mathbf{m}_{\mathbf{r}} \times \mathbf{m}_{\mathbf{r}+a\mathbf{e}_y}) + D \sum_{\mathbf{r}, i} \mathbf{e}_y \cdot (\mathbf{m}_{\mathbf{r}} \times \mathbf{m}_{\mathbf{r}+a\mathbf{e}_x})$. The spin dynamics is governed by the LLG equation:

$$\frac{d\mathbf{m}_{\mathbf{r}}}{dt} = -\gamma \mathbf{m}_{\mathbf{r}} \times \mathbf{H}_{\text{eff}} + \alpha \mathbf{m}_{\mathbf{r}} \times \frac{d\mathbf{m}_{\mathbf{r}}}{dt}, \quad (6)$$

where γ denotes the gyromagnetic ratio, α the Gilbert damping coefficient, $\mathbf{m}_{\mathbf{r}}$ the unit vector of magnetic moment, and $\mathbf{H}_{\text{eff}} = -\nabla_{\mathbf{m}_{\mathbf{r}}}(H/J)$ the effective magnetic field. Equation (6) is numerically integrated using the fourth-order Runge-Kutta method with a time step of Δt .

In our simulation, we define one unit of time as \hbar/J , corresponding to 0.505 ps for $J = 1.3$ meV and one unit of magnetic field density to 22.36 T. Hereafter, we set $\hbar = J = 1$ and nondimensionalize the other quantities. The following parameter values are used in the simulation: $\Delta t = 0.001$, $\gamma = 1$, $\alpha = 0.1$, $\omega = 0.285$ corresponding to about 0.09 THz and lattice constant $a = 1$.

Results—We first consider the magnetic fields of π -vector beams on the equator ($\theta = \pi/2$). Specifically, we study the magnetic response in two ferromagnetic systems that respectively stabilize Bloch skyrmions and

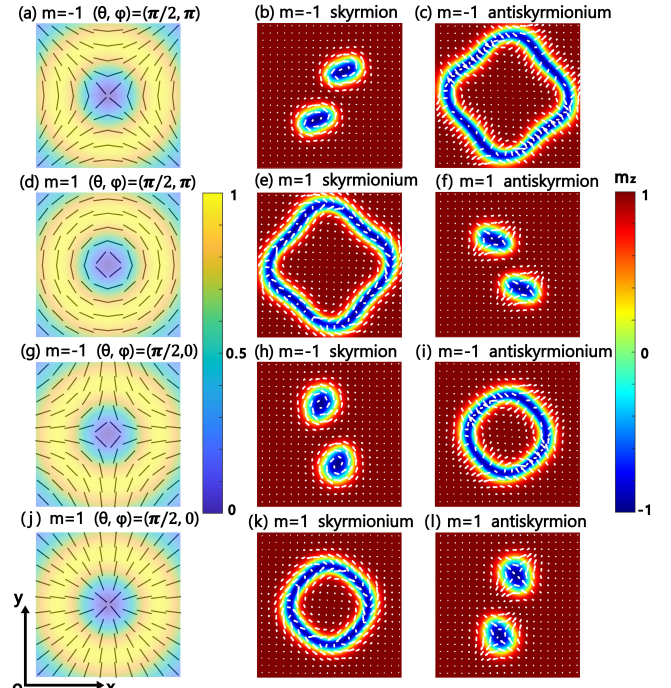


FIG. 2. Magnetization dynamics of the magnets under the influence of beams at $\theta = \pi/2$ on the HOPS with $m = \pm 1$. Snapshots of spin states for (a), (d), (g), (j) the magnetic fields in magnet possessing DMI that stabilizes (b), (e), (h), (k) Bloch skyrmions and (c), (f), (i), (l) antiskyrmions.

antiskyrmions via DMI, under the magnetic fields of two representative π -vector beams: the π -radial beam ($\varphi = 0$) and the π -azimuthal beam ($\varphi = \pi$). We set $W = 10a$, $t_0 = 7.72$, $\sigma = 2.57$, $D = 0.5$, $B_0 = 0.46$, and $H_z = 0.115$. In Fig. 2, we show the simulation results at $t = 129$.

Fig. 2(a) and (g) show the magnetic field and intensity distributions of the π -azimuthal vector beam at coordinates $(\pi/2, \pi)$ and $(\pi/2, 0)$ on the HOPS with $m = -1$, respectively. As shown before, these two magnetic field distributions exhibit similar configurations that can be interpreted as four vortex configurations. They can be applied to a magnet possessing DMI that stabilizes Bloch skyrmions, in both cases, inducing two skyrmions, as shown in Fig. 2(b) and (h), respectively; while a higher amplitude would yield four skyrmions due to the chirality interplay of light and magnetism [32]. Alternatively, the similar configurations can be viewed as a hollow core structure resembling the internal texture of an antiskyrmion (saddle surface), which leads to the formation of a single antiskyrmion in a magnet possessing DMI that stabilizes antiskyrmions, as shown in Fig. 2(c) and (i), respectively.

Fig. 2(d) and (j) show the magnetic field and intensity distributions of the magnetic field for the π -azimuthal vector beam at coordinates $(\pi/2, \pi)$ and $(\pi/2, 0)$ on the HOPS with $m = 1$, respectively. The corresponding magnetic field configuration in Fig. 2(d) can be interpreted

as a single hollow vortex. This magnetic field will induce a single skyrmion in a magnet possessing DMI that stabilizes Bloch skyrmions, as shown in Fig. 2(e). Alternatively, the same field can lead to the formation of two antiskyrmions in a magnet with antiskyrmion-stabilizing DMI, as shown in Fig. 2(f), while a higher amplitude would yield four antiskyrmions. Owing to the identical winding number, the corresponding magnetic field distribution in Fig. 2(j) excites similar phenomena in the magnet, as shown in Figs. 2(k) and (l).

By comparing Figs. 2(c) and (i), we observe that the antiskyrmionium generated in Fig. 2(c) is considerably larger than that in Fig. 2(i), indicating a stronger magnetic influence from the light in Fig. 2(a) on the magnet compared to that from Fig. 2(g). Similarly, the comparison between Figs. 2(e) and (k) also exhibits a similar phenomenon. This is due to the varying degree of matching between the magnetic polarization distribution of equatorial light (determined by φ) and the magnetization distribution of the in-plane components of the encoded (anti)skyrmions (determined by the helicity number [95, 96]). When $\varphi = 0$, the magnetic polarization distribution of the light is radial, as shown in Figs. 2(g) and (j). When $\varphi = \pi$, the magnetic polarization distribution of the light is rotated by $\pi/2$ compared to that at $\varphi = 0$, resulting in an azimuthal distribution, as shown in Figs. 2(a) and (d). Constrained by the form of the DMI, this study only encodes (anti)skyrmions with a helicity number of $\pi/2$. The magnetization distribution of this type of (anti)skyrmion matches the magnetic polarization distribution of light at $\varphi = \pi$. Therefore, the influence of the magnetic polarization distribution of light at $\varphi = \pi$ is stronger.

Next, we consider the magnetic fields of circularly and elliptically ($\theta \neq \pi/2$) polarized beams. As established previously, these beams share topological properties with equatorial beams and thus induce similar topological textures. In Fig. 3, we show the result of the magnetic effects induced by the optical fields at coordinates $(\pi, 0)$ and $(3\pi/4, 0)$ on the HOPSs for $m = \pm 1$ at $t = 129$ under the same conditions as above.

Figure 3(a) and (g) show the magnetic field and intensity distributions of the beams at coordinates $(\pi, 0)$ and $(3\pi/4, 0)$ on the HOPS with $m = -1$, respectively. They can induce two skyrmions, as shown in Fig. 3(b) and (h), and they can also induce a single antiskyrmionium, as shown in Fig. 3(c) and (i).

Figure 3(d) and (j) show the magnetic field and intensity distributions of the beams at coordinates $(\pi, 0)$ and $(3\pi/4, 0)$ on the HOPS with $m = 1$, respectively. They can encode a single skyrmionium, as shown in Fig. 3(e) and (k) and also encode two antiskyrmions, as shown in Fig. 3(f) and (l), while a higher amplitude would yield four antiskyrmions.

Based on the results from Figs. 2 and 3, we conclude that a HOPS of order m consists of lights with an identical winding number, which is given by $l = m$. The corresponding magnetic fields induce topological textures in

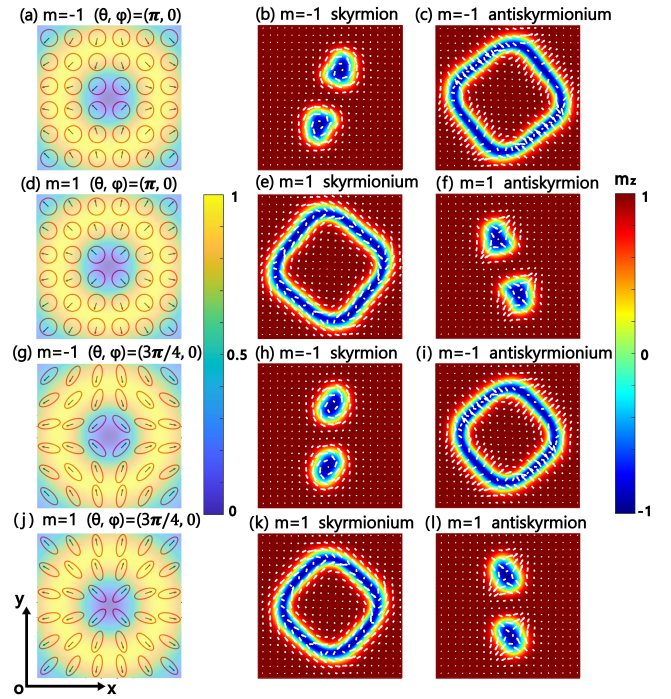


FIG. 3. Magnetization dynamics of the magnets under the influence of beams at $\theta = \pi$ and $3\pi/4$ on the HOPS with $m = \pm 1$. Snapshots of spin states for (a), (d), (g), (j) the magnetic fields in magnet possessing DMI that stabilizes (b), (e), (h), (k) Bloch skyrmions and (c), (f), (i), (l) antiskyrmions.

the magnet, which may exist as a single entity or multiple entities, with a total topological skyrmion number ranging from

$$Q_t = Q \cdot |Q_v \cdot m - 1| \sim 2Q \cdot |Q_v \cdot m - 1|. \quad (7)$$

Here, Q and Q_v denote the topological skyrmion number and vorticity number of a single skyrmion [95]. Q is given by [97]:

$$Q = \frac{1}{4\pi} \int d^2 \mathbf{r} [\mathbf{m}_r \cdot (\partial_x \mathbf{m}_r \times \partial_y \mathbf{m}_r)]. \quad (8)$$

In our simulations, a skyrmion possesses $Q = -1$ and $Q_v = +1$, whereas an antiskyrmion possesses $Q = +1$ and $Q_v = -1$. In a previous study, we have summarized the relationship between the total angular momentum \mathcal{J} of circularly polarized vortex light and Q_t of skyrmions induced in magnets, that is, from $Q_t = Q \cdot |\mathcal{J}|$ to $Q_t = 2Q \cdot |\mathcal{J}|$ [32]. This relationship holds for circularly polarized light, but itself is limited in that it cannot be extended to other polarization states on the HOPS.

To date, an all-optical method to encode skyrmion bags is not yet possible. Strikingly, our all-optical control method enables the encoding of two types of skyrmion bags: the $S_1(Q_{\text{bag}} + 1)$ type, with an outer skyrmion enclosing inner skyrmions [98] and the $S_2(|Q_{\text{bag}}|)$ type, with an outer closed domain enclosing inner skyrmions [99]. Q_{bag} represents the topological skyrmion number of the skyrmion bag.

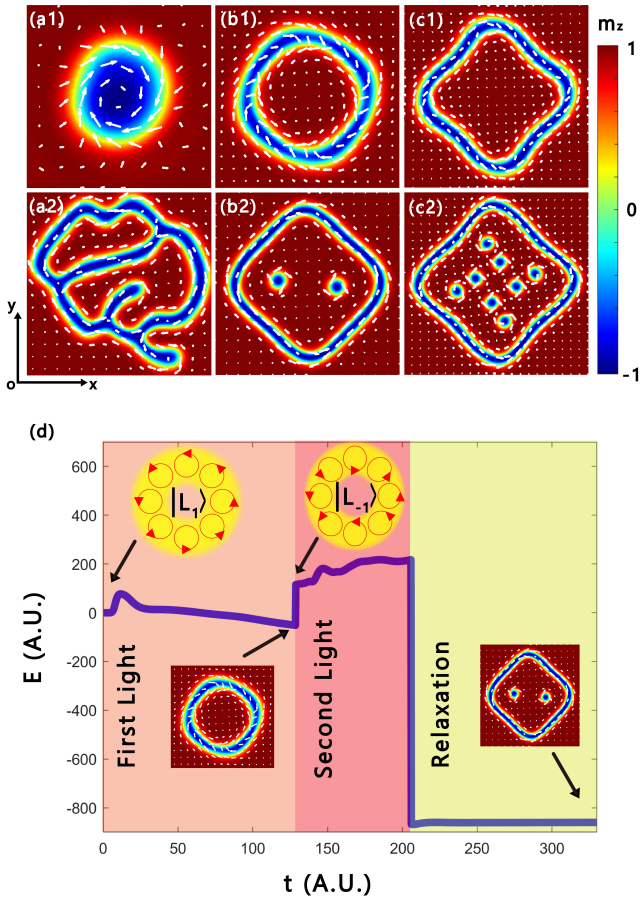


FIG. 4. Magnetization dynamics of magnet possessing DMI that stabilizes Bloch skyrmions under the influence of two kinds of HOPS beams. Snapshots of spin states in the magnet (a1) at $t = 78$ and (a2) in the stable state, which is skyrmion bag $S_1(2)$; Snapshots of spin states (b1) at $t = 129$ and (b2) in the stable state, which is skyrmion bag $S_2(2)$; Snapshots of spin states (c1) at $t = 208$ and (c2) in the stable state, which is skyrmion bag $S_2(8)$; (d) Energy-versus-time curve for the topological texture formation process shown in (b2).

Building on the above encoding principle, we propose a sequential excitation strategy: sequentially applying two HOPS beams to the magnet a skyrmion bag can be designed and encoded. In Fig. 4, we show the simulation about the encoding of skyrmion bags. Fig. 4(a1) shows the state of a single skyrmion generated in the magnet with $D = 0.615$ and $H_z = 0.06$ by a RCP beam with $W = 10a$, $B_0 = 0.58$, $t_0 = 7.72$, $\sigma = 2.57$ corresponding to the point $(0, 0)$ on a HOPS with $m = 0$, captured at $t = 78$. Subsequently, we use a π -radial vector beam with $W = 5a$, $B_0 = 0.19$, $t_0 = 10.29$, $\sigma = 5.14$ (corresponding to the point $(\pi/2, 0)$ on the HOPS with $m = -1$) into the pre-existing skyrmion. Since the skyrmion bag has negative formation energy, it may subsequently undergoes a stripe phase evolution to lower its energy, eventually transforming into stripe domains [51]. Thus, we increase the external magnetic field to arrest this energy-driven

evolution and stabilize the configuration. Specifically, at $t = 155$, we increase the external magnetic field to $H_z = 0.192$ and allow the system to relax. Finally, a stabilized skyrmion bag $S_1(2)$ is shown in Fig. 4(a2).

Further, Fig. 4(b1) shows the state of a single skyrmionium generated in the magnet with $D = 0.5$ and $H_z = 0.115$ by the LCP beam with $W = 10a$, $B_0 = 0.58$, $t_0 = 7.72$, $\sigma = 2.57$ corresponding to the point $(\pi, 0)$ on the HOPS with $m = 1$, captured at $t = 129$. We then irradiate this pre-existing skyrmionium with a π -radial vector beam (corresponding to the point $(\pi/2, 0)$ on the HOPS with $m = -1$) with $W = 10a$, $B_0 = 0.27$, $t_0 = 10.29$, $\sigma = 5.14$. Next, at $t = 206$, we increase the external magnetic field to $H_z = 0.192$ and allow the system to relax. Finally, stabilized skyrmion bag $S_2(2)$ is shown in Fig. 4(b2). We set the initial energy of the system to zero, and the energy evolution throughout the process is shown in Fig. 4(d), where the energy of the skyrmion bag eventually stabilizes. The energy evolution behaviors of all skyrmion bags in Fig. 4(a-c) are similar.

Our strategy can also be extended to the case with $|m| > 1$. However, the pre-existing skyrmionium in Fig. 4(b1) fractures under irradiation by a π -radial vector beam at $(\pi/2, 0)$, as the higher OAM increases the beam's effective area. Specifically, the resulting full coverage fractures the structure by forcing its internal moments to reorient. To prevent this, we first evolve the skyrmionium under the same configuration above until $t = 206$ in Fig. 4(c1). The skyrmionium exhibits a larger size and enhanced structural stability, making it less susceptible to fracturing upon subsequent optical excitation. The underlying mechanism for this size increase is its negative formation energy; to approach the energy minimum, it spontaneously expands and gradually develops striations, eventually evolving toward a stripe phase [51]. Subsequently, we applied a π -radial vector beam (with $W = 10a$, $B_0 = 0.46$, $t_0 = 10.29$, $\sigma = 5.14$) from the point $(\pi/2, 0)$ on the HOPS with $m = -3$. Next, at $t = 283$, we increase the external magnetic field to $H_z = 0.192$ and allow the systems to relax. Finally, a stabilized skyrmion bag $S_2(8)$ is shown in Fig. 4(c2). Videos illustrating the encoding of skyrmion bags in Fig. 4 can be found in the Supplemental Material.

Conclusion—In summary, we develop a theoretical framework that establishes a topological connection between structured light and magnetic texture. For any polarized light on the HOPS, the structured magnetic fields generated therefrom share similar topological properties and can encode varying numbers of skyrmions and antiskyrmions on two distinct types of DMI magnets that respectively host Bloch-type skyrmions and antiskyrmions. Specifically, when the order is m , topological textures with an absolute Q_t ranging from $Q \cdot |Q_v \cdot m - 1|$ to $2Q \cdot |Q_v \cdot m - 1|$ can be encoded. Furthermore, by sequentially applying two HOPS structured beams to the magnetic material, skyrmion bags with different Q_{bag} can be encoded.

Our all-optical method for encoding topological tex-

tures offers broader implications than previous findings that relied solely on circularly polarized light to generate skyrmions [32]. Here, the scope extends from circular polarization to any polarization on the HOPS, and from only skyrmions to both skyrmions and antiskyrmions. In contrast to the predominantly non-all-optical methods currently available [83, 86–88, 98, 99], we provide an all-optical alternative for encoding various types of skyrmion bags in magnetic materials. Our method offers enhanced convenience, efficiency, and flexibility.

Acknowledgment—S. Lin acknowledges the funding from National Natural Science Foundation of China

(Grant No. 12104296) and the startup funding from Great Bay University (No. YJKY220018). Y. Shen acknowledges the funding from Singapore Ministry of Education (MOE) AcRF Tier 1 grants (RG157/23 & RT11/23), Singapore Agency for Science, Technology and Research (A*STAR) MTC Individual Research Grants (M24N7c0080), and a Nanyang Assistant Professorship Start Up grant. Z. Nie acknowledges the funding from National Natural Science Foundation of China (Grants Nos. 12574333 and 11974258), Innovation Research Fundation of National University of Defense Technology (Grant No. 25-28).

[1] Andrew Forbes, Michael De Oliveira, and Mark R Dennis. Structured light. *Nature Photonics*, 15(4):253–262, 2021.

[2] Chao He, Yijie Shen, and Andrew Forbes. Towards higher-dimensional structured light. *Light: Science & Applications*, 11(1):205, 2022.

[3] Yijie Shen, Xuejiao Wang, Zhenwei Xie, Changjun Min, Xing Fu, Qiang Liu, Mali Gong, and Xiaocong Yuan. Optical vortices 30 years on: Oam manipulation from topological charge to multiple singularities. *Light: Science & Applications*, 8(1):90, 2019.

[4] Giovanni Milione, HI Sztul, DA Nolan, and RR Alfano. Higher-order poincaré sphere, stokes parameters, and the angular momentum of light. *Physical review letters*, 107(5):053601, 2011.

[5] Qiwen Zhan. Properties of circularly polarized vortex beams. *Optics letters*, 31(7):867–869, 2006.

[6] Sumit Ghosh, Stefan Blügel, and Yuriy Mokrousov. Ultrafast optical generation of antiferromagnetic meron-antimeron pairs with conservation of topological charge. *Physical Review Research*, 5(2):L022007, 2023.

[7] Benoit Truc, Alexey A Sapozhnik, Phoebe Tengdin, Emil Viñas Boström, Thomas Schönenberger, Simone Gargiulo, Ivan Madan, Thomas LaGrange, Arnaud Magrez, Claudio Verdozzi, et al. Light-induced metastable hidden skyrmion phase in the mott insulator cu2oseo3. *Advanced Materials*, 35(33):2304197, 2023.

[8] Yutao Tang, Kingfai Li, Xuecai Zhang, Junhong Deng, Guixin Li, and Etienne Brasselet. Harmonic spin-orbit angular momentum cascade in nonlinear optical crystals. *Nature Photonics*, 14(11):658–662, 2020.

[9] Shirong Lin, LuoJia Wang, Luqi Yuan, and Xianfeng Chen. All-optical control of the photonic hall lattice in a pumped waveguide array. *Physical Review Applied*, 17(6):064029, 2022.

[10] Jian Chen, Chenhao Wan, and Qiwen Zhan. Engineering photonic angular momentum with structured light: a review. *Advanced Photonics*, 3(6):064001–064001, 2021.

[11] Qinmiao Chen, Geyang Qu, Jun Yin, Yuhang Wang, Ziheng Ji, Wenhong Yang, Yujie Wang, Zhen Yin, Qinghai Song, Yuri Kivshar, et al. Highly efficient vortex generation at the nanoscale. *Nature Nanotechnology*, 19(7):1000–1006, 2024.

[12] Feng Mei, Geyang Qu, Xinbo Sha, Jing Han, Moxin Yu, Hao Li, Qinmiao Chen, Ziheng Ji, Jincheng Ni, Cheng-Wei Qiu, et al. Cascaded metasurfaces for high-purity vortex generation. *Nature Communications*, 14(1):6410, 2023.

[13] Wenrui Miao, Yongtao Zhang, and Greg Gbur. Deterministic vortices evolving from partially coherent fields. *Optica*, 10(9):1173–1176, 2023.

[14] Sicong Wang, Zhikai Zhou, Zecan Zheng, Jialin Sun, Hongkun Cao, Shichao Song, Zi-Lan Deng, Fei Qin, Yaoyu Cao, and Xiangping Li. Topological structures of energy flow: Poynting vector skyrmions. *Physical Review Letters*, 133(7):073802, 2024.

[15] Shirong Lin, Zhongquan Nie, Weichao Yan, Yao Liang, Han Lin, Qing Zhao, and Baohua Jia. All-optical vectorial control of multistate magnetization through anisotropy-mediated spin-orbit coupling. *Nanophotonics*, 8(12):2177–2188, 2019.

[16] Mauro Fanciulli, Matteo Pancaldi, Anda-Elena Staniciu, Matthieu Guer, Emanuele Pedersoli, Dario De Angelis, Primož Rebernik Ribič, David Bresteau, Martin Luttmann, Pietro Carrara, et al. Magnetic vortex dynamics probed by time-resolved magnetic helicoidal dichroism. *Physical Review Letters*, 134(15):156701, 2025.

[17] Jaeyu Kim, Seungmo Yang, Dongha Kim, Kyoung-Woong Moon, Changsoo Kim, Chanyong Hwang, and Min-Kyo Seo. Photothermal skyrmion tweezer: programmable optical manipulation of magnetic topological quasiparticles. *Nature Communications*, 16(1):11375, 2025.

[18] Marco Finazzi, Matteo Savoini, AR Khorsand, A Tsukamoto, A Itoh, Lamberto Duo, Andrei Kirilyuk, Th Rasing, and M Ezawa. Laser-induced magnetic nanostructures with tunable topological properties. *Physical Review Letters*, 110(17):177205, 2013.

[19] Yao Guang, Iuliia Bykova, Yizhou Liu, Guoqiang Yu, Eberhard Goering, Markus Weigand, Joachim Gräfe, Se Kwon Kim, Junwei Zhang, Hong Zhang, et al. Creating zero-field skyrmions in exchange-biased multilayers through x-ray illumination. *Nature communications*, 11(1):949, 2020.

[20] Sayed Ali Akbar Ghorashi and Qiang Li. Dynamical generation of higher-order spin-orbit coupling, topology, and persistent spin texture in light-irradiated altermagnets. *Phys. Rev. Lett.*, 135:236702, 2025.

[21] Koki Nukui, Satoshi Iihama, Kazuaki Ishibashi, Soma Miki, Luding Wang, and Shigemi Mizukami. Light helicity-induced torques in metallic magnets. *Journal of*

the Physical Society of Japan, 94(11):111002, 2025.

[22] Zongxia Guo, Junlin Wang, Gregory Malinowski, Boyu Zhang, Wei Zhang, Hangtian Wang, Chen Lyu, Yi Peng, Pierre Vallobra, Yong Xu, et al. Single-shot laser-induced switching of an exchange biased antiferromagnet. *Advanced Materials*, 36(21):2311643, 2024.

[23] Sicong Wang, Chen Wei, Yuanhua Feng, Hongkun Cao, Wenzhe Li, Yaoyu Cao, Bai-Ou Guan, Arata Tsukamoto, Andrei Kirilyuk, Alexey V Kimel, et al. Dual-shot dynamics and ultimate frequency of all-optical magnetic recording on gdfeco. *Light: Science & Applications*, 10(1):8, 2021.

[24] Wei Zhang, Michel Hehn, Yi Peng, Jon Gorchon, Quentin Remy, Jun Xiao Lin, Julius Hohlfeld, Grégoire Malinowski, Wei Sheng Zhao, and Stéphane Mangin. Deterministic ultra-fast all-optical switching in gd free ferrimagnetic spin valve structures. *Advanced Functional Materials*, page e05423, 2025.

[25] Xuefeng Wu, Xu Li, Wenyu Kang, Xichao Zhang, Li Chen, Zhibai Zhong, Yan Zhou, Johan Åkerman, Yaping Wu, Rong Zhang, et al. Topology-induced chiral photon emission from a large-scale meron lattice. *Nature Electronics*, 6(7):516–524, 2023.

[26] Benjamin Assouline and Amir Capua. Faraday effects emerging from the optical magnetic field. *Scientific Reports*, 15(1):39566, 2025.

[27] Masahiro Sato, Shintaro Takayoshi, and Takashi Oka. Laser-driven multiferroics and ultrafast spin current generation. *Phys. Rev. Lett.*, 117:147202, 2016.

[28] Benjamin Assouline and Amir Capua. Helicity-dependent optical control of the magnetization state emerging from the landau-lifshitz-gilbert equation. *Physical Review Research*, 6(1):013012, 2024.

[29] Jian Zhou and Chunmei Zhang. Contrasting light-induced spin torque in antiferromagnetic and altermagnetic systems. *Physical Review Letters*, 134(17):176902, 2025.

[30] AO Leonov, TL Monchesky, N Romming, A Kubetzka, AN Bogdanov, and R Wiesendanger. The properties of isolated chiral skyrmions in thin magnetic films. *New Journal of Physics*, 18(6):065003, 2016.

[31] Hiroyuki Fujita and Masahiro Sato. Encoding orbital angular momentum of light in magnets. *Physical Review B*, 96(6):060407, 2017.

[32] Qifan Zhang, Shirong Lin, and Wu Zhang. Skyrmion generation through the chirality interplay of light and magnetism. *Communications Physics*, 2026. doi: 10.1038/s42005-026-02488-9.

[33] Sougata Mallick, Peng Ye, Willem Boutu, David Gauthier, Hamed Merdji, Manuel Bibes, Michel Viret, Karim Bouzehouane, and Vincent Cros. OAM driven nucleation of sub-50 nm compact antiferromagnetic skyrmions. *Advanced Functional Materials*, 34(49):2409528, 2024.

[34] Sayantika Bhowal and Nicola A Spaldin. Magnetoelectric classification of skyrmions. *Physical Review Letters*, 128(22):227204, 2022.

[35] X-G Wang, Levan Chotorlishvili, Nikita Arnold, VK Dugaev, Igor Maznichenko, J Barnaś, PA Buczek, Stuart SP Parkin, and Arthur Ernst. Plasmonic skyrmion lattice based on the magnetoelectric effect. *Physical Review Letters*, 125(22):227201, 2020.

[36] Kaixin Zhu, Linzhu Bi, Yongzhao Zhang, Dingguo Zheng, Dong Yang, Jun Li, Huanfang Tian, Jianwang Cai, Huaixin Yang, Ying Zhang, et al. Ultrafast switching to zero field topological spin textures in ferrimagnetic tbfecos films. *Nanoscale*, 16(6):3133–3143, 2024.

[37] Kathinka Gerlinger, Bastian Pfau, Felix Büttner, Michael Schneider, Lisa-Marie Kern, Josefina Fuchs, Deter Engel, Christian M Günther, Mantao Huang, Ivan Lemesh, et al. Application concepts for ultrafast laser-induced skyrmion creation and annihilation. *Applied Physics Letters*, 118(19), 2021.

[38] Zizhao Gong, Wei Zhang, Jianan Liu, Zongkai Xie, Xu Yang, Jin Tang, Haifeng Du, Na Li, Xiangqun Zhang, Wei He, and Zhao-hua Cheng. Ultrafast demagnetization dynamics in the epitaxial fege(111) film chiral magnet. *Phys. Rev. B*, 107:144429, 2023.

[39] Mana Miyata, Jun-ichiro Ohe, and Gen Tatara. Topological charge control of skyrmion structure in frustrated magnets by circularly polarized light. *Physical Review Applied*, 18(1):014075, 2022.

[40] Hanqing Shi, Jingwei Zhang, Yilian Xi, Heping Li, Jingyi Chen, Iftikhar Ahmed, Zhijie Ma, Ningyan Cheng, Xiang Zhou, Haonan Jin, et al. Dynamic behavior of above-room-temperature robust skyrmions in 2d van der waals magnet. *Nano Letters*, 24(36):11246–11254, 2024.

[41] XC Hu, XS Wang, HY Yuan, and XR Wang. Recent progress in magnetic skyrmion morphology. *Reviews in Physics*, page 100111, 2025.

[42] Wanjun Jiang, Xichao Zhang, Guoqiang Yu, Wei Zhang, Xiao Wang, M Benjamin Jungfleisch, John E Pearson, Xuemei Cheng, Olle Heinonen, Kang L Wang, et al. Direct observation of the skyrmion hall effect. *Nature Physics*, 13(2):162–169, 2017.

[43] Tomek Schulz, R Ritz, Andreas Bauer, Madhumita Halder, Martin Wagner, Chris Franz, Christian Pfeiferer, Karin Everschor, Markus Garst, and Achim Rosch. Emergent electrodynamics of skyrmions in a chiral magnet. *Nature Physics*, 8(4):301–304, 2012.

[44] Hao Wu, Felix Groß, Bingqian Dai, David Lujan, Seyed Armin Razavi, Peng Zhang, Yuxiang Liu, Kemał Sobotkiewich, Johannes Förster, Markus Weigand, et al. Ferrimagnetic skyrmions in topological insulator/ferrimagnet heterostructures. *Advanced Materials*, 32(34):2003380, 2020.

[45] Takehito Yokoyama and Jacob Linder. Josephson effect through magnetic skyrmions. *Physical Review B*, 92(6):060503, 2015.

[46] Eric Mascot, Jasmin Bedow, Martin Graham, Stephan Rachel, and Dirk K Morr. Topological superconductivity in skyrmion lattices. *npj Quantum Materials*, 6(1):6, 2021.

[47] Andrew Hardy, Anjishnu Bose, Tanmay Grover, and Arun Paramekanti. Charge ordering and spontaneous topological hall effect in bilayer skyrmion crystals. *Phys. Rev. B*, 111:115115, 2025.

[48] Takaaki Dohi, Mona Bhukta, Fabian Kammerbauer, Venkata Krishna Bharadwaj, Ricardo Zarzuela, Aakanksha Sud, Maria-Andromachi Syskaki, Duc Minh Tran, Thibaud Denneulin, Sebastian Wintz, et al. Observation of a non-reciprocal skyrmion hall effect of hybrid chiral skyrmion tubes in synthetic antiferromagnetic multilayers. *Nature Communications*, 16(1):8285, 2025.

[49] Fengshan Zheng, Nikolai S Kiselev, Filipp N Rybakov, Luyan Yang, Wen Shi, Stefan Blügel, and Rafal E Dunin-Borkowski. Hopfion rings in a cubic chiral magnet. *Nature*, 623(7988):718–723, 2023.

[50] Zhejunyu Jin, Zhaozhuo Zeng, Yunshan Cao, and Peng Yan. Skyrmion hall effect in altermagnets. *Physical Review Letters*, 133(19):196701, 2024.

[51] XR Wang, XC Hu, and HT Wu. Stripe skyrmions and skyrmion crystals. *Communications Physics*, 4(1):142, 2021.

[52] XS Wang, HY Yuan, and XR Wang. A theory on skyrmion size. *Communications Physics*, 1(1):31, 2018.

[53] Haitao Wu, Xuchong Hu, Keyu Jing, and XR Wang. Size and profile of skyrmions in skyrmion crystals. *Communications Physics*, 4(1):210, 2021.

[54] XR Wang, Xu-Chong Hu, and Zhou-Zhou Sun. Topological equivalence of stripy states and skyrmion crystals. *Nano Letters*, 23(9):3954–3962, 2023.

[55] OJ Amin, SF Poole, S Reimers, LX Barton, A Dal Din, F Maccherozzi, SS Dhesi, Vít Novák, F Krizek, JS Chauhan, et al. Antiferromagnetic half-skyrmions electrically generated and controlled at room temperature. *Nature Nanotechnology*, 18(8):849–853, 2023.

[56] Felix Büttner, Bastian Pfau, Marie Böttcher, Michael Schneider, Giuseppe Mercurio, Christian M Günther, Piet Hessing, Christopher Klose, Angela Wittmann, Kathinka Gerlinger, et al. Observation of fluctuation-mediated picosecond nucleation of a topological phase. *Nature Materials*, 20(1):30–37, 2021.

[57] Wataru Koshibae and Naoto Nagaosa. Creation of skyrmions and antiskyrmions by local heating. *Nature Communications*, 5(1):5148, 2014.

[58] Tomoyuki Yokouchi, Satoshi Sugimoto, Bivas Rana, Shinichiro Seki, Naoki Ogawa, Shinya Kasai, and Yoshichika Otani. Creation of magnetic skyrmions by surface acoustic waves. *Nature Nanotechnology*, 15(5):361–366, 2020.

[59] Maya Khela, Maciej Dąbrowski, Safe Khan, Paul S Keatley, Ivan Verzhbitskiy, Goki Eda, Robert J Hicken, Hidekazu Kurebayashi, and Elton JG Santos. Laser-induced topological spin switching in a 2d van der waals magnet. *Nature communications*, 14(1):1378, 2023.

[60] Tim Titze, Sabri Koraltan, Timo Schmidt, Dieter Suess, Manfred Albrecht, Stefan Mathias, and Daniel Steil. All-optical control of bubble and skyrmion breathing. *Physical review letters*, 133(15):156701, 2024.

[61] Zefang Li, Huai Zhang, Guanqi Li, Jianguo Guo, Qingping Wang, Ying Deng, Yue Hu, Xuange Hu, Can Liu, Minghui Qin, et al. Room-temperature sub-100 nm néel-type skyrmions in non-stoichiometric van der waals ferromagnet fe3-x gate2 with ultrafast laser writability. *Nature Communications*, 15(1):1017, 2024.

[62] Roméo Juge, Naveen Sisodia, Joseba Urrestarazu Larrañaga, Qiang Zhang, Van Tuong Pham, Kumi Gaurav Rana, Brice Sarpi, Nicolas Mille, Stefan Stanescu, Rachid Belkhou, et al. Skyrmions in synthetic antiferromagnets and their nucleation via electrical current and ultra-fast laser illumination. *Nature Communications*, 13(1):4807, 2022.

[63] Alexander Samardak, Alexander Kolesnikov, Maksim Stebliy, Ludmila Chebotkevich, Alexandr Sadovnikov, Sergei Nikitov, Abhishek Talapatra, Jyoti Mohanty, and Alexey Ognev. Enhanced interfacial dzyaloshinskii-moriya interaction and isolated skyrmions in the inversion-symmetry-broken ru/co/w/ru films. *Applied Physics Letters*, 112(19), 2018.

[64] Bei Ding, Yadong Wang, Jiahui Meng, Xuejin Wan, Qingping Wang, Xinxing Xu, Yu Zhu, Minghui Qin, Xingsen Gao, Xiaoyan Zhong, et al. Multistep skyrmion phase transition driven by light-induced uniaxial strain. *Science Advances*, 11(20):eadt2698, 2025.

[65] Dhritiman Bhattacharya, Seyed Armin Razavi, Hao Wu, Bingqian Dai, Kang L Wang, and Jayasimha Atulasimha. Creation and annihilation of non-volatile fixed magnetic skyrmions using voltage control of magnetic anisotropy. *Nature Electronics*, 3(9):539–545, 2020.

[66] Long Li, Dongsheng Song, Weiwei Wang, Lingyao Kong, Shuisen Zhang, Ning Wang, Shilei Zhang, Mingliang Tian, Jiadong Zang, Yizhou Liu, and Haifeng Du. Electrically writing a magnetic heliknoton in a chiral magnet. *Nature Materials*, 2026. doi:10.1038/s41563-025-02450-0.

[67] Jiwen Chen, Laichuan Shen, Hongyu An, Xichao Zhang, Hua Zhang, Haifeng Du, Xiaoguang Li, and Yan Zhou. Magnetic bimeron traveling on the domain wall. *Applied Physics Letters*, 126(14), 2025.

[68] Jantje Kalin, Sibylle Sievers, HW Schumacher, R Abram, H Füser, M Bieler, D Kalin, A Bauer, and C Pfleiderer. Optical creation and annihilation of skyrmion patches in a chiral magnet. *Physical Review Applied*, 21(3):034065, 2024.

[69] Zhuolin Li, Qiangwei Yin, Wenxin Lv, Jun Shen, Shouguo Wang, Tongyun Zhao, Jianwang Cai, Hechang Lei, Shi-Zeng Lin, Ying Zhang, et al. Electron-assisted generation and straight movement of skyrmion bubble in kagome tbmn6sn6. *Advanced Materials*, 36(19):2309538, 2024.

[70] Haonan Jin, Jingyi Chen, Gerrit van der Laan, Thorsten Hesjedal, Yizhou Liu, and Shilei Zhang. Rolling motion of rigid skyrmion crystallites induced by chiral lattice torque. *Nano Letters*, 24(39):12226–12232, 2024.

[71] Nirel Bernstein, Hang Li, Benjamin Assouline, Yong-Chang Lau, Igor Rozhansky, Wenhong Wang, and Amir Capua. Spin-torque skyrmion resonance in a frustrated magnet. *Nature Communications*, 16(1):4616, 2025.

[72] Vladyslav M Kuchkin, Bruno Barton-Singer, Pavel F Bessarab, and Nikolai S Kiselev. Symmetry-governed dynamics of magnetic skyrmions under field pulses. *Communications Physics*, 8(1):26, 2025.

[73] Maarten A Brems, Tobias Sparmann, Simon M Fröhlich, Leonie-C Dany, Jan Rothörl, Fabian Kammerbauer, Elizabeth M Jefremovas, Oded Farago, Mathias Kläui, and Peter Virnau. Realizing quantitative quasiparticle modeling of skyrmion dynamics in arbitrary potentials. *Physical Review Letters*, 134(4):046701, 2025.

[74] Linjie Liu, Fei Sun, Jianhua Ren, Weijin Chen, and Yue Zheng. Dynamics of magnetic skyrmions under steady and time-varying deformation. *Reports on Progress in Physics*, 88(9):096501, 2025.

[75] Kaiying Dou, Wenhui Du, Zhonglin He, Ying Dai, Baibiao Huang, and Yandong Ma. Ultrafast laser driven ferromagnetic-antiferromagnetic skyrmion switching in 2d topological magnet. *Small*, 21(11):2412320, 2025.

[76] Na Cai and Yan Liu. Acceleration and deceleration behavior of skyrmion controlled by curvature gradient in elliptical-ring track. *Advanced Electronic Materials*, 10(10):2400080, 2024.

[77] Callum R MacKinnon, Katharina Zeissler, Simone Finizio, Jörg Raabe, Christopher H Marrows, Tim Mercer, Philip R Bissell, and Serban Lepadatu. Collective skyrmion motion under the influence of an additional interfacial spin-transfer torque. *Scientific Reports*, 12(1):10786, 2022.

[78] Laichuan Shen, Jing Xia, Xichao Zhang, Motohiko Ezawa, Oleg A Tretiakov, Xiaoxi Liu, Guoping Zhao, and Yan Zhou. Current-induced dynamics and chaos of anti-ferromagnetic bimerons. *Physical review letters*, 124(3):037202, 2020.

[79] Heng Niu, Han Gyu Yoon, Hee Young Kwon, Zhiyuan Cheng, Siqi Fu, Hongying Zhu, Bingfeng Miao, Liang Sun, Yizheng Wu, Andreas K Schmid, et al. Magnetic skyrmionic structures with variable topological charges in engineered dzyaloshinskii-moriya interaction systems. *Nature Communications*, 16(1):3453, 2025.

[80] Dongxing Yu, Yonglong Ga, Jinghua Liang, Chenglong Jia, and Hongxin Yang. Voltage-controlled dzyaloshinskii-moriya interaction torque switching of perpendicular magnetization. *Physical Review Letters*, 130(5):056701, 2023.

[81] Yu Li, Leonardo Pierobon, Michalis Charilaou, Hans-Benjamin Braun, Niels R Walet, Jörg F Löfli, James J Miles, and Christoforos Moutafis. Tunable terahertz oscillation arising from bloch-point dynamics in chiral magnets. *Physical Review Research*, 2(3):033006, 2020.

[82] Philipp N Rybakov and Nikolai S Kiselev. Chiral magnetic skyrmions with arbitrary topological charge. *Physical review B*, 99(6):064437, 2019.

[83] David Foster, Charles Kind, Paul J Ackerman, Jung-Shen B Tai, Mark R Dennis, and Ivan I Smalyukh. Two-dimensional skyrmion bags in liquid crystals and ferromagnets. *Nature Physics*, 15(7):655–659, 2019.

[84] XR Wang and XC Hu. Particle-continuum duality of skyrmions. *Physical Review B*, 107(17):174412, 2023.

[85] Hai-Tao Wu, Xu-Chong Hu, and XR Wang. Nematic and smectic stripe phases and stripe-skx transformations. *Science China Physics, Mechanics & Astronomy*, 65(4):247512, 2022.

[86] Luyan Yang, Andrii S Savchenko, Fengshan Zheng, Nikolai S Kiselev, Philipp N Rybakov, Xiaodong Han, Stefan Blügel, and Rafal E Dunin-Borkowski. Embedded skyrmion bags in thin films of chiral magnets. *Advanced materials*, 36(36):2403274, 2024.

[87] Jialiang Jiang, Yaodong Wu, Lingyao Kong, Yongsen Zhang, Sheng Qiu, Huanhuan Zhang, Yajiao Ke, Shouguo Wang, Mingliang Tian, and Jin Tang. Stable néel-twisted skyrmion bags in a van der waals magnet fe3-x gate2 at room temperature. *Nano Letters*, 25(8):3282–3290, 2025.

[88] Quan Liu, Shouzhe Dong, Yutong Wang, Junhang Liu, Guofu Xu, Hua Bai, Hao Bai, Weideng Sun, Zhiying Cheng, Yunjie Yan, et al. Room-temperature creation and conversion of individual skyrmion bags in magnetic multilayered disks. *Nature Communications*, 16(1):125, 2025.

[89] Albert Fert, Vincent Cros, and Joao Sampaio. Skyrmions on the track. *Nature nanotechnology*, 8(3):152–156, 2013.

[90] Bingqian Dai, Tianyi Wang, Albert Lee, Shijie Xu, Zhongjian Bian, Xinyue Zhu, Puyang Huang, Aadi Chaturvedi, Yaochen Li, Yang Cheng, et al. Transient antiskyrmion-mediated topological transitions in isotropic magnets. *Advanced Science*, page e13126, 2026.

[91] Xiao-Ping Ma, Kangjie Tian, Qi-Shuo Wang, Xiao-Xue Yang, Huiting Li, Je-Ho Shim, Hongyan Zhang, Zhaochu Luo, and Hong-Guang Piao. Domain-wall-isolated dual-lane racetrack for crosstalk-free skyrmion propagation. *Applied Physics Letters*, 127(25), 2025.

[92] Yuhan Chang, Hongyuan Hao, Huiliang Wu, Yalu Zuo, Hao Wu, Zhipeng Hou, Guoqiang Yu, Xiaoxi Liu, Li Xi, Senfu Zhang, et al. Suppressed skyrmion hall effect of hybrid magnetic skyrmions by helicity engineering. *Advanced Functional Materials*, page 2421771, 2025.

[93] Alexander P Petrović, Christina Psaroudaki, Peter Fischer, Markus Garst, and Christos Panagopoulos. Colloquium: Quantum properties and functionalities of magnetic skyrmions. *Reviews of Modern Physics*, 97(3):031001, 2025.

[94] Christian Back, Vincent Cros, Hubert Ebert, Karin Everschor-Sitte, Albert Fert, Markus Garst, Tianping Ma, Sergiy Mankovsky, TL Monchesky, Maxim Mostovoy, et al. The 2020 skyrmionics roadmap. *Journal of Physics D: Applied Physics*, 53(36):363001, 2020.

[95] Xichao Zhang, Yan Zhou, Kyung Mee Song, Tae-Eon Park, Jing Xia, Motohiko Ezawa, Xiaoxi Liu, Weisheng Zhao, Guoping Zhao, and Seonghoon Woo. Skyrmion-electronics: writing, deleting, reading and processing magnetic skyrmions toward spintronic applications. *Journal of Physics: Condensed Matter*, 32(14):143001, 2020.

[96] Xiaoyan Yao and Shuai Dong. Vector vorticity of skyrmionic texture: An internal degree of freedom tunable by magnetic field. *Phys. Rev. B*, 105:014444, 2022.

[97] Sanyum Channa, Houssam Sabri, Xin Yu Zheng, Tian-Yue Chen, Haowen Ren, Qiuchen Wu, Kun Wang, Yun-tian Li, Zbigniew Galazka, Ian R Fisher, et al. Signatures of fluctuation-driven magnetic topological charge in p-ferromagnetic insulator bilayers. *Physical Review Letters*, 135(9):096702, 2025.

[98] Lan Bo, Rongzhi Zhao, Chenglong Hu, Xichao Zhang, Xuefeng Zhang, and Masahito Mochizuki. Controllable creation of skyrmion bags in a ferromagnetic nanodisk. *Physical Review B*, 107(22):224431, 2023.

[99] Lisa-Marie Kern, Vladyslav M Kuchkin, Victor Deinhart, Christopher Klose, Themistoklis Sidiropoulos, Maike Auer, Simon Gaebel, Kathinka Gerlinger, Riccardo Battistelli, Steffen Wittrock, et al. Controlled formation of skyrmion bags. *Advanced Materials*, page 2501250, 2025.